JOURNAL OF MATERIALS SCIENCE 26 (1991) 5815–5822

Coprecipitation-derived mullite and mullite-zirconia composites

S. RAJENDRAN*, H. J. ROSSELL
CSIRO, Division of Materials Science and Technology, Locked Bag 33, Clayton, Victoria 3168, Australia

Precursor powders of mullite–zirconia (0–40 wt% ZrO_2) were prepared by a hydroxide coprecipitation method and their behaviour during calcination between room temperature and 1500 °C was studied using thermal analysis, X-ray diffraction and electron microscopy. The only crystalline phases present in the precalcined powders were bayerite and gibbsite, and these were stable up to 250 °C. Powders containing ZrO_2 were initially amorphous, but on calcination between 250 and 850 °C produced different crystalline phases at temperatures which depended on the amount of zirconia present. Thus in the case of mullite–40 wt% ZrO_2, zirconia crystallized at about 850 °C and was stable up to 1200 °C, when it reacted with free silica to form zircon ($ZrSiO_4$). Mullite formed above 1250 °C at the expense of zircon and remained stable at higher temperatures. The oxide powders were very homogeneous, and on sintering produced ceramics with a fine-grained uniform microstructure. The powders were very reactive and could be sintered conventionally to near-theoretical density at 1600–1700 °C without sintering aids. The fracture strength of mullite was about 275 MPa, and this could be improved to 350 MPa by hot isostatic pressing the presintered bodies. Addition of zirconia enhanced the sintering kinetics as well as the fracture strength of mullite.

1. Introduction

Mullite ($3Al_2O_3 \cdot 2SiO_2$) is a technically attractive material because it has a low thermal expansion (5.0×10^{-6}) [1], high melting point (1850 °C) [1], good hardness and chemical stability, and excellent high-temperature creep resistance [2]. Conventional fabrication of mullite involves the heating of mechanically mixed component oxides to at least 1500 °C to effect reaction and homogenization. Further heating for long periods above about 1700 °C, perhaps with the use of sintering aids, is required for densification [3]. The resulting coarse-grained and often porous mullite bodies are mechanically weak, while the high-temperature mechanical properties are severely degraded due to the presence of glassy grain boundary phases which can arise from silica inhomogeneities and from sintering aids.

In an effort to improve the properties of mullite, other fabrication methods such as hot pressing [4] and hot isostatic pressing [5] have been investigated. Also, a number of chemical methods [4–14] including coprecipitation, hydrolytic decomposition of mixed metal alkoxides, and colloidal and polymeric gel techniques have been employed to produce homogeneous, unagglomerated, reactive mullite powder. In addition, zirconia has been incorporated into mullite to improve the mechanical properties [15–25]. Reaction sintering of alumina and zircon to mullite and zirconia [15–18] is an attractive process, but the reaction is difficult to control, resulting in poor reproducibility of properties and microstructures in the sintered bodies.

In the course of studies on yttria partially-stabilized zirconia (Y-PSZ) and Y-PSZ–Al_2O_3 composites [26, 27], a coprecipitation technique was developed to produce readily sinterable, reactive fine powders. This technique has been extended to other systems including alumina and alumina–zirconia [28]. In this paper, characterization of mullite and mullite–zirconia powders is reported, with studies of their sintering behaviour: microstructures and mechanical properties of sintered bodies are referred to, but will be reported in more detail elsewhere.

2. Experimental procedures

The required amounts of standard solutions of AR aluminium nitrate in water (2.0 M), tetramethoxy orthosilicate in methanol (0.15 ml/ml of methanol), and zirconyl nitrate (0.5 M ZrO_2, prepared by dissolving zirconium oxycarbonate in nitric acid) were mixed and added to rapidly stirred AR ammonia solution to produce coprecipitated hydrated oxides. The precipitates were filtered, washed free of salts, twice dispersed ultrasonically in acetone and dried in a vacuum oven at 75 °C for 24 h. These oven-dried powders were calcined at temperatures between 75

*Present address: Advanced Materials Programme, Australian Nuclear Science and Technology Organisation, Private Mail Bag 1, Menai, New South Wales 2234, Australia.

0022–2461/91 $03.00 + .12

and 1400 °C for 2 h in most of the work described below.

Differential thermal analyses (DTA) were carried out using a Stanton–Redcroft derivatograph operated from 20–1400 °C at a heating rate of 10 °C min^{-1}, and with 10-mg samples.

Powder X-ray diffraction (XRD) patterns were recorded with a Rigaku diffractometer using filtered CuK_α radiation and a scanning rate of 2°(2Θ) min^{-1}. Diffraction patterns of some specimens were recorded on film using a Guinier–Lenné camera operating with Cu$K_{\alpha 1}$ radiation. This device can produce a continuous photographic record of the diffraction pattern as the specimen is heat-treated according to a desired programme in the range 20–1500 °C. Heating rates of 50 °C h^{-1} and a film speed of 1 mm h^{-1} usually were necessary for satisfactory exposures.

Transmission electron microscopy was done with a Joel 100CX microscope operated at 100 kV. Samples for TEM were prepared by allowing an aqueous suspension to dry on grids coated with carbon film. Oxide powders, prepared by calcining the precursor powders between 1100 and 1350 °C for 2 h, were compressed isostatically and sintered in the range 1500–1700 °C for 2 h. Such (conventionally) sintered materials were occasionally treated further by hot isostatic pressing (HIPing) at 1500 °C for 30 min in argon at 200 MPa. Bulk densities of the sintered bodies were determined by a mercury displacement method. Microstructures of the polished and thermally etched bodies were examined in a scanning electron microscope. Fracture strength measurements were made using a three-point bend apparatus with a 12.5-mm outer span and a 0.05 mm min^{-1} crosshead speed.

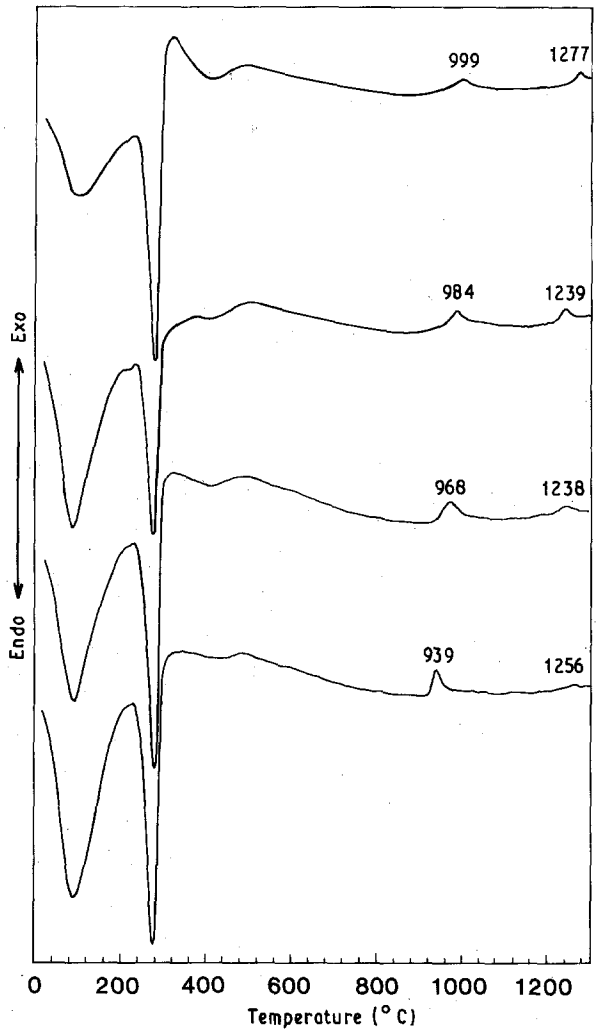

Figure 1 Differential thermal analysis (DTA) curves of coprecipitated mullite–zirconia precursor powders. (a) M-00ZrO_2, (b) M-10ZrO_2, (c) M-20ZrO_2 and (d) M-30ZrO_2.

3. Results and discussion

Characterization procedures were applied to both the oven-dried precursor powders and calcined powders, i.e. precursor material heat-treated for 2 h. Mullite–zirconia materials are referred to as M-$xx$$ZrO_2$, where xx is the wt % of ZrO_2 in the composite.

3.1. Thermal analysis

DTA curves of mullite and mullite–zirconia coprecipitated precursors are given in Fig. 1. All the curves have three endothermic and two exothermic peaks. The first (lowest temperature) endotherm can be explained as due to the removal of loosely-bound adsorbed water: although the material was carefully dried initially, it has a very large specific surface area, and so water adsorption occurs immediately on exposure to the atmosphere. The other two endotherms are due to the removal of chemically-bonded water, i.e. the conversion of hydrous oxides and hydroxides of Si, Al and Zr to their respective oxides. These assignments are consistent with the weight changes that occurred during each endothermic event (TGA curves, not shown).

There is no remarkable difference in any of these DTA curves up to 800 °C, apart from expected variance in endothermic peak height, which indicates that the constituents of the powder are homogeneously distributed. If hydrous zirconia is distributed inhomogeneously in a matrix of hydrous alumina–silica, its dehydration will occur separately from that of alumina, and may lead to yet another endothermic event [29].

It has been explained elsewhere [30] that the exothermic DTA peaks that occur on heating powders of mullite composition are due to the decomposition of a small amount of aluminosilicate and/or the γ-Θ transformation of alumina at 1000 °C, and also to the formation of mullite at about 1280 °C. The presence of zirconia influences the crystallization behaviour of the aluminosilicate, as can be seen in Fig. 1. Further, X-ray and electron diffraction studies (see below) showed that the exotherm near 1000 °C was due to the crystallization of ZrO_2 and not to that of any alumina or silica component.

3.2. X-ray Diffraction

XRD patterns from the oven-dried samples (M-$xx$$ZrO_2$–75 °C, recorded at room temperature) showed the presence of at least three phases; bayerite, gibbsite and an amorphous phase, the presence of

which was indicated by a broad diffuse diffraction peak at about $d = 0.30$ nm. The proportion of bayerite and gibbsite increased, while that of the amorphous phase decreased with increasing zirconia content of the specimens. Samples which had been calcined between 250 and 900 °C were all amorphous to X-rays, but after calcination at 1000 and 1100 °C followed by cooling, specimens M-$xx$$ZrO_2$, $xx > 0$, all contained cubic or tetragonal zirconia. The aluminosilicate species which must be present remained amorphous to X-rays.

XRD patterns of materials heated at 1350 °C for 2 h and cooled are shown in Fig. 2. The pattern for the zirconia-free specimen corresponds to that expected

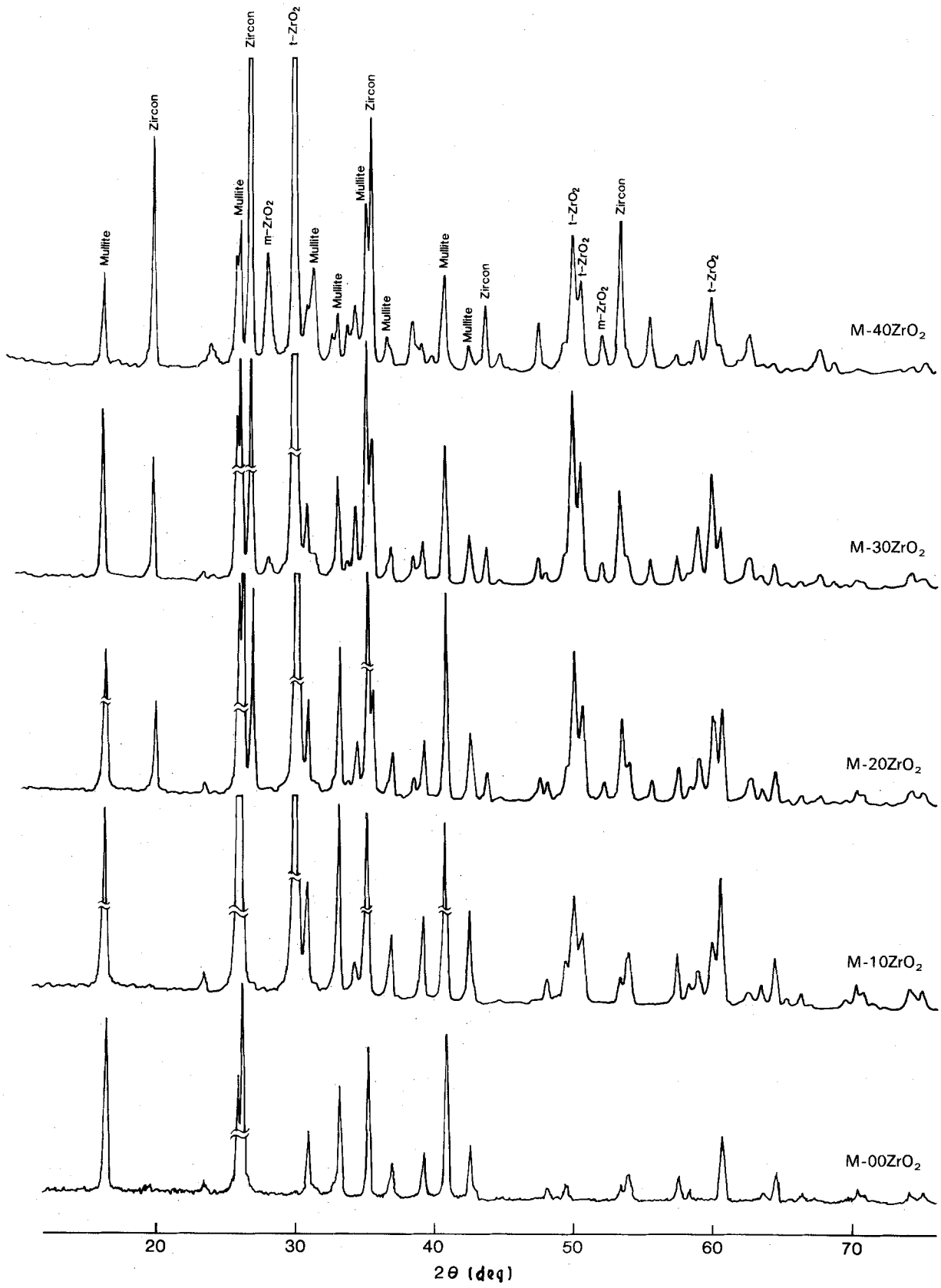

Figure 2 Powder XRD patterns of mullite and mullite–zirconia calcined at 1350 °C for 2 h.

for mullite of composition $3Al_2O_3 \cdot 2SiO_2$, while that for M-10ZrO_2 shows the presence of both tetragonal zirconia and mullite. Specimens M-$xx$$ZrO_2$, $xx > 10$, when calcined at 1350 °C and cooled contained zircon ($ZrSiO_4$), monoclinic ZrO_2, tetragonal ZrO_2 and mullite. It can be seen from the intensities of the diffraction peaks in Fig. 2 that as the zirconia content of the specimens increases, the proportions of mullite and tetragonal ZrO_2 decrease, while those of monoclinic ZrO_2 and zircon increase. Therefore it is evident that the aluminosilicate species crystallizes as mullite and zircon between 1100 and 1350 °C if zirconia is present, and that the formation of zircon is favoured over that of mullite, at least at the lower temperatures. However, specimens calcined above 1500 °C have XRD patterns for mullite and zirconia phases only.

The Guinier–Lenné photographs gave XRD results in agreement with those above. Thus during heating the precursor powder M-40ZrO_2 from room temperature, bayerite and gibbsite were the only detectable crystalline phases up to 240 °C, at which temperature the background intensity rose sharply, indicating that the specimen had become amorphous. No crystalline phases were apparent on further heating until 850 °C, when the background intensity abruptly decreased, and very broad lines due to cubic zirconia (crystallite size 6–10 nm) appeared. These lines sharpened due to crystallite growth as the temperature was raised, and the zirconia transformed to the tetragonal form at 1080 °C. The tetragonal ZrO_2 crystals continued to grow as the temperature increased: by 1220 °C the lines were very sharp, indicating a crystal size of 1 μm. At this temperature, zircon began to form as very small crystals, and at 1260 °C mullite also began to form. The proportions of mullite and zirconia increased at the expense of the zircon at about 1350 °C, and at 1430 °C, no zircon remained.

Unfortunately, above about 1400 °C reaction of the silica in mullite with the platinum specimen holder occurred, so that specimens were converted to alumina and zirconia (and Pt_2Si). However, these XRD results show that at no stage during the calcination of these powders above 250 °C do alumina or silica appear as separate crystalline phases; the alumina in particular remains in a cryptocrystalline or amorphous condition until it reacts with zircon and/or amorphous silica to form mullite at relatively high temperature.

3.3. Electron microscopy

A detailed TEM study of the pure mullite precursor (i.e. M-00ZrO_2) during calcination has been reported [30]. Typical electron micrographs of the oven-dried precursor powders M-$xx$$ZrO_2$ are given in Fig. 3. These show that ZrO_2 seems to have no effect on the microstructure. Thus the major identifiable component is $Al(OH)_3$ in irregular, spongy plates, and there

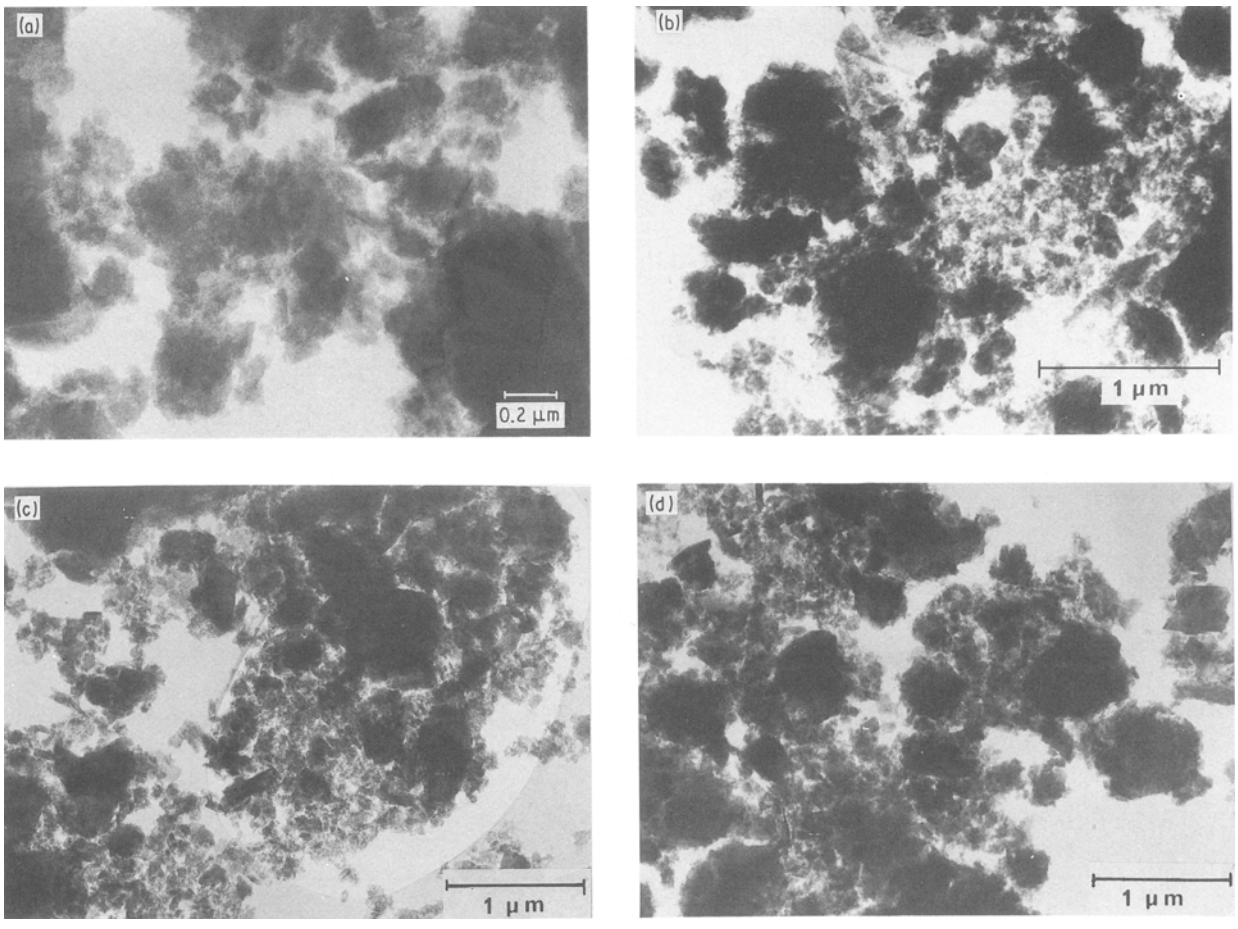

Figure 3 Transmission electron micrographs (TEM) of oven-dried mullite–zirconia coprecipitated powders. (a) M-00ZrO_2, (b) M-10ZrO_2, (c) M-20ZrO_2 and (d) M-30ZrO_2.

are occasional relatively large and well-formed rectangular crystals of gibbsite and bayerite, and small crystals of an unidentified phase.

Zirconia-containing specimens heated between 250 and 900 °C appeared as a spongy amorphous material. This morphology was unchanged with increasing temperature in the range and with increasing zirconia content, and so appeared the same as that observed for the oven-dried materials. The presence of zirconia could not be identified in any of the specimens calcined up to 900 °C, despite the fact that TEM is far more sensitive than XRD for this purpose.

Crystalline zirconia could be detected in specimens calcined for 2 h at 1100 °C by electron diffraction; however, the technique could not distinguish between the cubic and tetragonal forms (Fig. 4). The accompanying micrographs show that the overall morphology differs little from that displayed by materials calcined at lower temperatures, and that the zirconia crystallites are angular, approximately equiaxed and distributed very uniformly through the alumina–silica matrix. The size of the zirconia crystals increased as the overall zirconia content increased, as would be expected: in the case of specimens with low zirconia

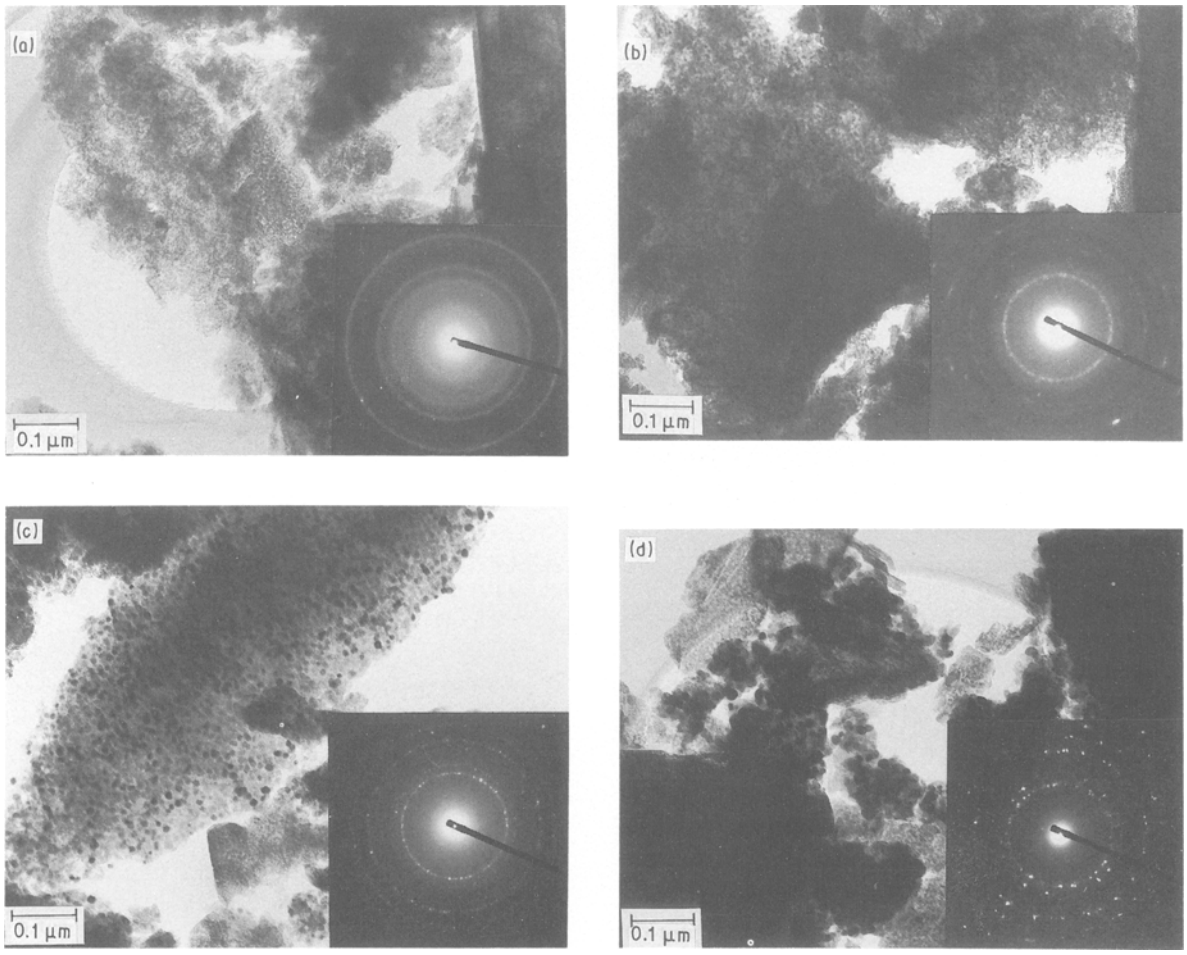

Figure 4 TEM of mullite–zirconia powders calcined at 1100 °C for 2 h. (a) M-00ZrO_2, (b) M-20ZrO_2, (c) M-30ZrO_2 and (d) M-40ZrO_2.

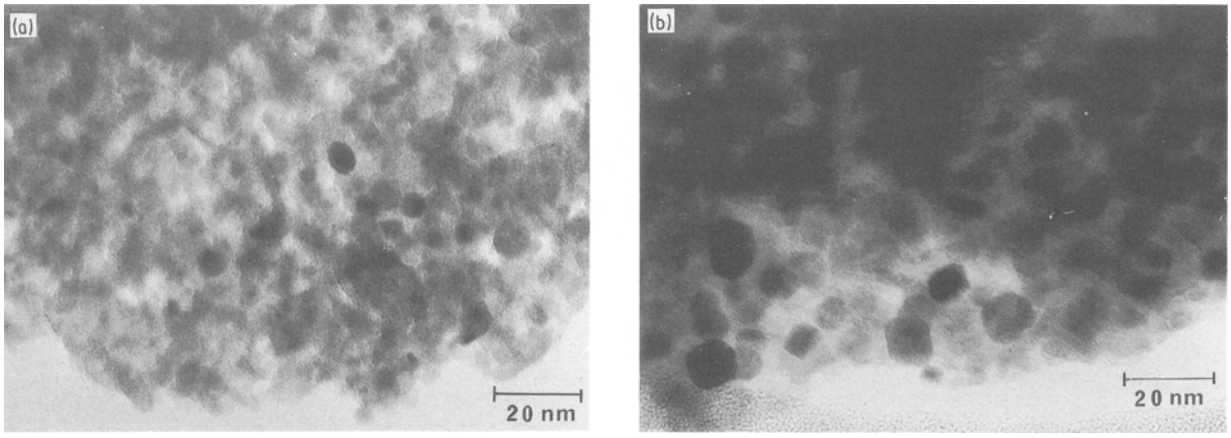

Figure 5 TEM of (a) M-10ZrO_2 and (b) M-20ZrO_2 powders after calcination at 1100 °C for 2 h.

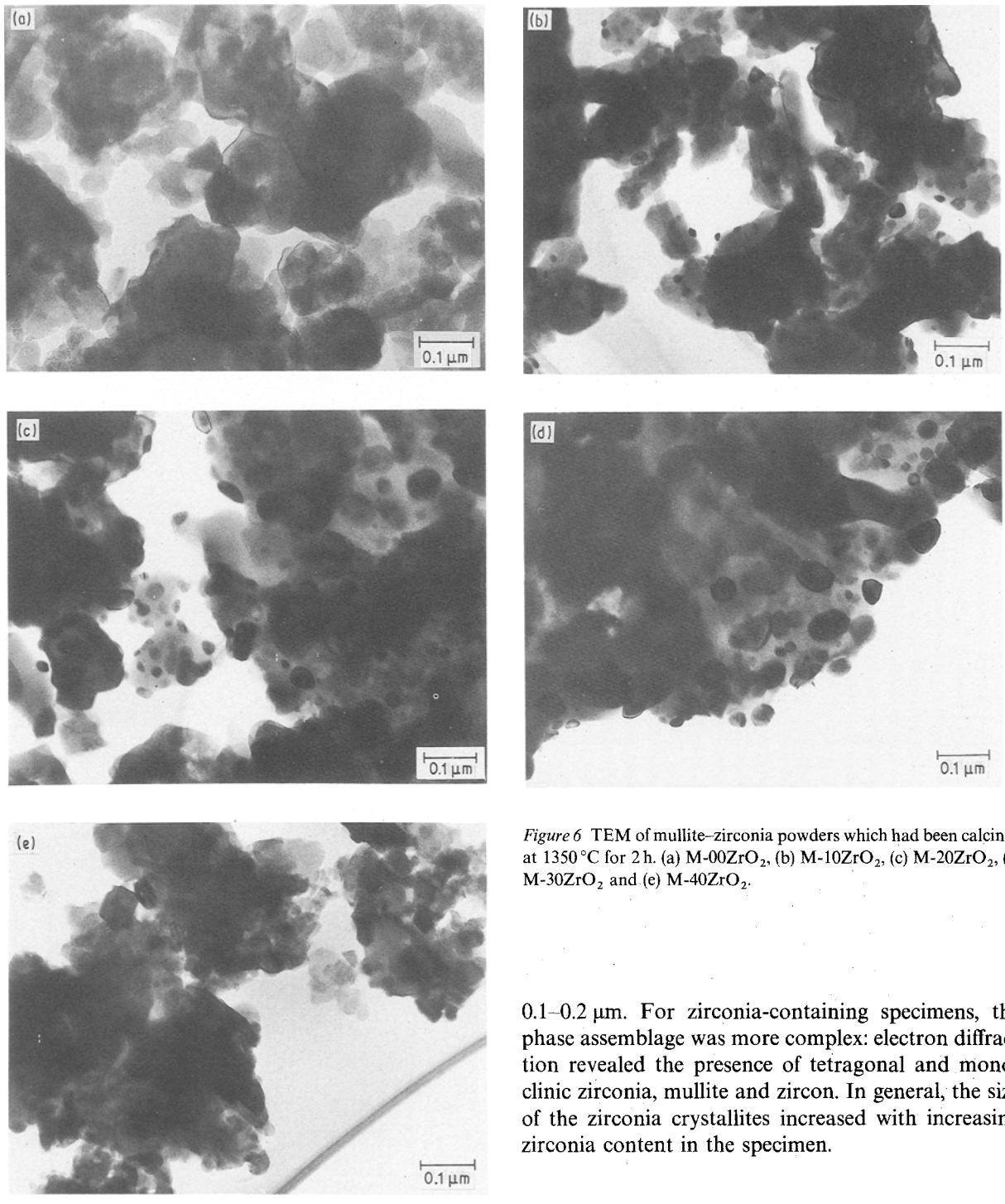

Figure 6 TEM of mullite–zirconia powders which had been calcined at 1350 °C for 2 h. (a) M-00ZrO_2, (b) M-10ZrO_2, (c) M-20ZrO_2, (d) M-30ZrO_2 and (e) M-40ZrO_2.

content, the crystallites were obvious only at high magnification (Fig. 5). This effect is displayed also in the diffraction rings corresponding to zirconia, which become more spotty with increasing zirconia content of the specimen. It must be noted that the diffraction rings for the zirconia-free specimen are due to Θ-alumina, and that these rings are greatly attenuated or absent for specimens containing zirconia, suggesting that the presence of zirconia hinders the crystallization of alumina.

The morphology of specimens changed markedly after calcination at 1350 °C for 2 h (Fig. 6), and the nature of these changes could be associated with the zirconia content. The zirconia-free material consisted of polycrystalline mullite with a crystallite size of 0.1–0.2 μm. For zirconia-containing specimens, the phase assemblage was more complex: electron diffraction revealed the presence of tetragonal and monoclinic zirconia, mullite and zircon. In general, the size of the zirconia crystallites increased with increasing zirconia content in the specimen.

3.4. Sintering behaviour, microstructures and mechanical properties

The measured bulk densities (expressed as a percentage of the theoretical value) of mullite and mullite–zirconia specimens that had been sintered conventionally at 1600–1700 °C for 2 h are given in Fig. 7a. The bulk density of mullite increased from 2.02 to 3.14 g cm^{-3} for sintering temperatures in the range 1500–1700 °C: complete densification could be achieved only at temperatures > 1650 °C. Mullite of > 99% theoretical density could be made by HIPing (200 MPa, 1500 °C, 30 min) material previously sintered conventionally at 1650 °C, or by hot pressing the starting powder (30 MPa, uniaxial, 1500 °C, 30 min). Hot-pressed or HIPed bodies were translucent.

The addition of zirconia favourably influences the sintering kinetics of mullite (Fig. 7a), especially at

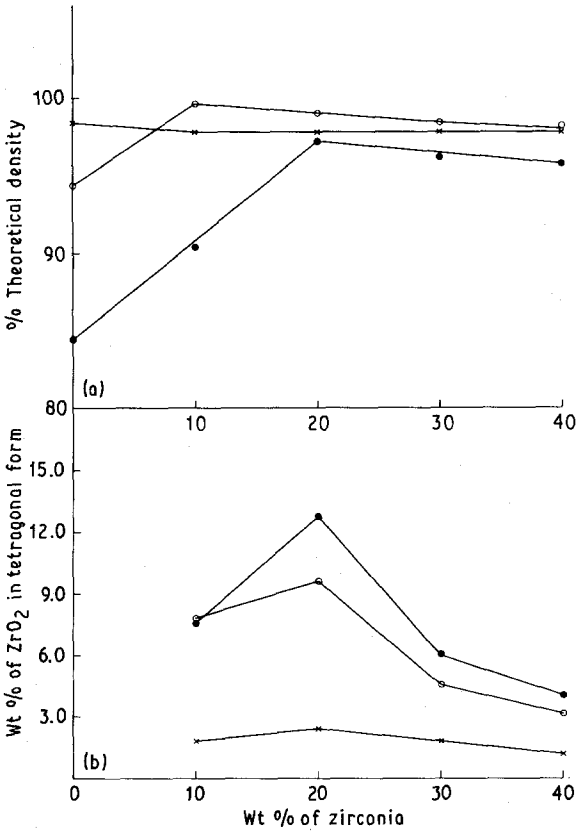

Figure 7 Mullite–zirconia composites sintered in the range 1600–1700 °C: (a) bulk density, as a percentage of theoretical density, and (b) fraction of zirconia retained in the tetragonal form on cooling (from XRD on polished specimens). ●, 1600; ○, 1650; ×, 1700 °C.

lower temperatures. The minimum temperature required for these composites to densify fully is at least 50 °C lower than that required for mullite alone. This effect has been reported before [19, 22, 24, 31], but it seems that the basic mechanism is not fully understood.

A degradation in measured bulk densities occurs for composites of zirconia content > 20 wt % that have been sintered at temperatures > 1650 °C. Most of the zirconia in such specimens is in the monoclinic form (Fig. 7b), a consequence of the enhanced growth of zirconia crystals to sizes beyond that critical maximum for the retention of the tetragonal form on cooling. Theoretical densities were calculated using the observed proportions of monoclinic and tetragonal zirconia, so that the degradation in density is due probably to microcracks produced around those zirconia particles which transform spontaneously from the tetragonal to the monoclinic form (with consequent volume increase) on cooling.

Scanning electron micrographs of these materials are shown in Fig. 8. The pure mullite contains a proportion of large grains in an otherwise uniform fine-grained matrix. These large grains show well-developed facets, a morphology usually associated with the presence of glassy silica-based phases during growth [19]. In the composites, grain size is more uniform, and there is a uniform distribution of zirconia which is mainly intergranular, although a small proportion of zirconia dispersed intragranularly in mullite was observed in specimens sintered above

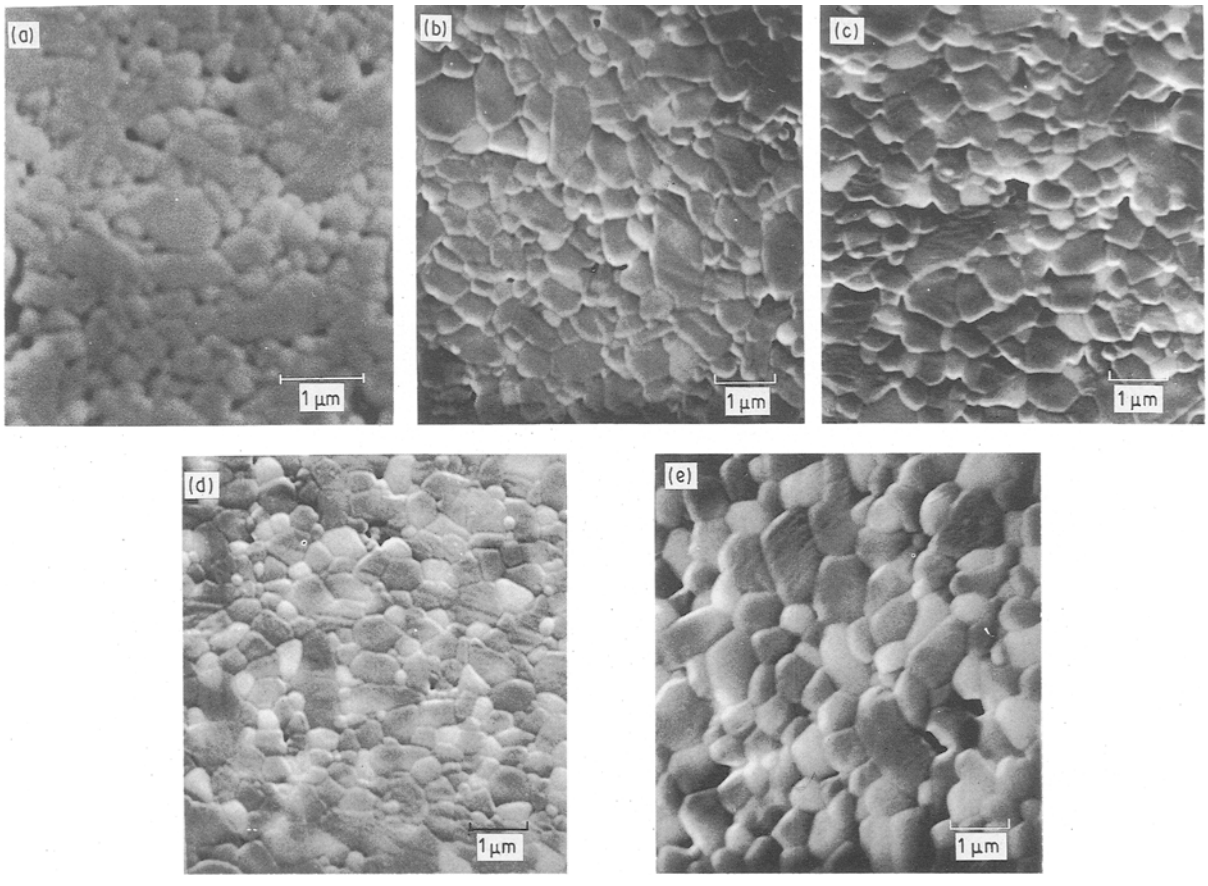

Figure 8 Scanning electron micrographs of polished and thermally etched millite–zirconia composites sintered at 1600 °C for 2 h. (a) M-00ZrO_2, (b) M-10ZrO_2, (c) M-20ZrO_2, (d) M-30ZrO_2 and (e) M-40ZrO_2.

TABLE I Fracture strength, σ(MPa) of mullite and mullite–zirconia specimens sintered previously to 1500–1700 °C

Samples	Sintering temperature for 2 h (°C)			
	1600	1650	1700	
M-00ZrO_2	–	265	275	
M-00ZrO_2	175	340	335	HIPed
M-00ZrO_2	350	?	?	hot-pressed
M-10ZrO_2	210	350	258	
M-20ZrO_2	350	415	295	
M-30ZrO_2	310	325	325	
M-40ZrO_2	290	385	255	

1600 °C. There is a gradual increase in the grain size of zirconia with increasing zirconia content of the composites.

Fracture strengths of the sintered and hot-pressed materials are given in Table I. These results are discussed in detail elsewhere [29], but some features are relevant here. The fracture strength of the conventionally sintered pure mullite is comparable to many reported values [13, 32, 33], while the increase in strength on hot-pressing or HIPing can be attributed mainly to the smaller grain size (< 0.5 μm) achieved by these procedures.

The addition of zirconia improved the fracture strength of mullite, with optimum strengthening occurring at about 20–30 wt % ZrO_2. The highest average value (415 MPa) may be compared to the 500 MPa achieved by Kubata and Takagi [15], and with strengths reported for similar material prepared by different processes, such as from very active powders (290 MPa) [20], reaction sintering (310 MPa) [23], *in situ* reaction (400 MPa) [17] and spray pyrolysis (360 MPa) [16]. The main reason the sintered mullite–zirconia materials produced here have relatively high strengths is that the bodies are dense, and have a nearly uniform grain size and a well-distributed second phase.

These properties are a consequence of the evolution of the original powders on calcination: by the time sintering temperatures are reached, the powders consist of fine (i.e. sinter-active) mullite particles in which a uniform distribution of zirconia crystallites has been established. It is probable that the mechanical properties of these materials could be enhanced through careful control of the calcination and sintering conditions to optimize the microstructures. Such optimization could include control of the size of the zirconia crystallites in order to confer a measure of toughness on the materials through the mechanisms of microcracking [19, 34] and stress-induced transformation of retained tetragonal zirconia [35].

Acknowledgements

The authors thank Mr G. L. Tan and Mr David Watson for technical help.

Received 30 July 1990
and accepted 6 February 1991

References

1. R. F. DAVIS and J. A. PASK, in "High Temperature Oxides", Part iv, edited by A. M. Alper (Academic Press, New York, 1971) p. 37.
2. P. A. LESSING, R. S. GORDON and K. S. MAZDIYASNI, *J. Amer. Ceram. Soc.* **58** (1975) 149.
3. M. D. SACKS and J. A. PASK, *ibid.* **65** (1982) 65.
4. K. S. MAZDIYASNI and L. M. BROWN, *ibid.* **55** (1972) 548.
5. S. PROCHAZKA and F. J. KLUG, *ibid.* **66** (1983) 874.
6. R. ROY, *ibid.* **39** (1956) 145.
7. A. G. ELLIT and R. A. HUGGINS, *ibid.* **58** (1975) 497.
8. M. S. J. GANI and R. McPHERSON, *J. Mater. Sci.* **12** (1977) 999.
9. T. A. WHEAT, E. M. H. SALLAM and A. C. D. CHALADER, *Ceramurgia Int.* **5** (1979) 42.
10. B. E. YOLDAS, *Amer. Ceram. Soc. Bull.* **59** (1980) 479.
11. G. Y. MENG and R. A. HUGGINS, *Mater. Res. Bull.* **18** (1983) 581.
12. D. W. HOFFMAN, R. ROY and S. KOMARNENI, *J. Amer. Ceram. Soc.* **67** (1984) 468.
13. S. KANZAKI, H. TABATA, T. KUMAZAWA and S. OHTA, *ibid.* **68** (1985) C6.
14. P. E. PEBELY, E. A. BARRINGER and H. K. BOWEN, *ibid.* **68** (1985) C76.
15. Y. KUBATA and N. TAKAGI, in "Special Ceramics", British Ceramic Proceedings, Vol. 8, edited by S. P. Hawlett and D. Taylor (Institute of Ceramics, Staffordshire, 1986) p. 179.
16. E. D. RUPO, T. G. CARUTHERS and R. J. BROOK, *J. Amer. Ceram. Soc.* **61** (1978) 69.
17. N. CLAUSSEN and J. JAHN, *ibid.* **63** (1980) 228.
18. J. S. WALLCE, N. CLAUSSEN, M. RUHLE and G. PETZOW, in "Materials Science Research", Vol. 14, edited by J. A. Pask and A. Evans (Plenum, New York, 1980) p. 155.
19. S. PROCHAZKA, J. S. WALLACE and N. CLAUSSEN, *J. Amer. Ceram. Soc.* **66** (1983) C125.
20. M. I. OSENDI, P. MIRANZO and J. S. MOYA, *J. Mater. Sci. Lett.* **2** (1983) 599.
21. G. D. PORTU and J. W. HENNEY, *Trans. Brit. Ceram. Soc.* **83** (1984) 69.
22. J. S. MOYA and M. I. OSENDI, *J. Mater. Sci.* **19** (1984) 2909.
23. P. BOCH and J. P. GIRY, *J. Mater. Sci. Engng* **71** (1985) 39.
24. Q. YUAN, J. TAN and Z. JIN, *J. Amer. Ceram. Soc.* **69** (1986) 265.
25. M. ISHITSUKA, T. SATO, T. ENDO and M. SHIMADA, *ibid.* **70** (1987) C342.
26. S. RAJENDRAN, M. V. SWAIN and H. J. ROSSELL, *J. Mater. Sci.* **23** (1988) 1805.
27. S. RAJENDRAN, J. V. SANDERS and H. J. ROSSELL, *ibid.* **24** (1989) 1195.
28. S. RAJENDRAN and H. J. ROSSELL, *Mater. Sci. Forum* **34–36** (1988) 549.
29. S. RAJENDRAN, Accepted *J. Mater. Sci.*
30. S. RAJENDRAN, H. J. ROSSELL and J. V. SANDERS *J. Mater. Sci* 25 (1990) 4462.
31. J. P. MORAN, T. KELLY, S. M. LAWLOR and J. A. SLEVIN, *Key Engng Mater.* **32** (1989) 57.
32. T. KAWANAMI, in "Mullite", edited by S. Somiya (Uchida Rokakuho Publishing Company, Tokyo, 1984) p. 123.
33. M. G. M. U. ISMAIL, Z. NAKAI and S. SOMIYA, *J. Amer. Ceram. Soc.* **70** (1987) C7.
34. N. CLAUSSEN, *ibid.* **59** (1976) 49.
35. M. RÜHLE, N. CLAUSSEN and A. H. HEUER, *ibid.* **69** (1986) 195.